Comparative Lipidomics Profiling of Human Atherosclerotic Plaques

Christin Stegemann, PhD; Ignat Drozdov, MSc; Joseph Shalhoub, BSc, MBBS, MRCS; Julia Humphries, PhD; Christophe Ladroue, PhD; Athanasios Didangelos, PhD; Mark Baumert, BSc; Mark Allen, PhD; Alun H. Davies, MA, DM, FRCS, FHEA; Claudia Monaco, MD, PhD; Alberto Smith, PhD; Qingbo Xu, MD, PhD; Manuel Mayr, MD, PhD

Background—We sought to perform a systematic lipid analysis of atherosclerotic plaques using emerging mass spectrometry techniques.

Methods and Results—A chip-based robotic nanoelectrospray platform interfaced to a triple quadrupole mass spectrometer was adapted to analyze lipids in tissue sections and extracts from human endarterectomy specimens by shotgun lipidomics. Eighteen scans for different lipid classes plus additional scans for fatty acids resulted in the detection of 150 lipid species from 9 different classes of which 24 were detected in endarterectomies only. Further analyses focused on plaques from symptomatic and asymptomatic patients and stable versus unstable regions within the same lesion. Polyunsaturated cholesteryl esters with long-chain fatty acids and certain sphingomyelin species showed the greatest relative enrichment in plaques compared to plasma and formed part of a lipid signature for vulnerable and stable plaque areas in a systems-wide network analysis. In principal component analyses, the combination of lipid species across different classes provided a better separation of stable and unstable areas than individual lipid classes.

Conclusions—This comprehensive analysis of plaque lipids demonstrates the potential of lipidomics for unraveling the lipid heterogeneity within atherosclerotic lesions. **(*Circ Cardiovasc Genet*. 2011;4:232-242.)**

Key Words: atherosclerosis ■ endarterectomy carotid ■ mass spectrometry ■ lipids ■ metabolomics

According to the response-to-retention hypothesis, the binding of cholesterol-containing lipoprotein particles to intimal proteoglycans is the central pathogenic process in atherogenesis.[1] Once retained, lipoproteins get oxidized, accumulate in "foam cells," and provoke a cascade of inflammatory processes that drive the formation of atherosclerosis and ultimately define the propensity of the plaque to rupture. In most studies, the lipid content in plaques is just visualized by oil red O staining. A more detailed characterization, including the detection of single lipid species rather than lipid classes, may provide a better classification of atherosclerotic lesions with the goal of illuminating biology and discovering clinical biomarkers.[2,3]

Editorial see p 215
Clinical Perspective on p 242

Although the potential of mass spectrometry (MS) has long been recognized,[4] it is the recent progress in MS technologies that has transformed our ability to profile atherosclerotic plaques by allowing the quantitation of hundreds of individual lipid species in complex biological samples.[5,6] For example, a recent study demonstrated that lipids in murine lesions can be imaged by multiplex coherent antistokes Raman spectroscopy.[3] Another study applied desorption electrospray ionization MS to image and identify 26 distinct lipid species in a single human plaque.[7] To our knowledge, an MS-based analysis comparing different human atherosclerotic lesions has not been reported to date. To reveal a characteristic lipid signature for plaque vulnerability, we took advantage of the latest MS developments in shotgun lipidomics and compared radial arteries, endarterectomy samples from symptomatic and asymptomatic patients, and stable and unstable areas within the same symptomatic lesion.

Methods

Clinical Samples

The study was approved by the Research Ethics Committees of King's College London and Imperial College London. All patients gave written informed consent. Surgical samples were derived from carotid or femoral endarterectomies and radial arteries. In total, 26 patients were included in this study. Their clinical characteristics are

Received November 25, 2010; accepted April 7, 2011.

From the King's British Heart Foundation Centre, King's College, London, UK (C.S., I.D., J.H., A.D., A.S., Q.X., M.M.); Kennedy Institute (J.S., C.M.) and Vascular Unit (A.H.D.), Imperial College, London, UK; University of Warwick, Coventry, UK (C.L.); and Advion Biosciences, Ltd, Norwich, UK (M.B., M.A.).

The online-only Data Supplement is available at http://circgenetics.ahajournals.org/cgi/content/full/CIRCGENETICS.110.959098/DC1.

Correspondence to Manuel Mayr, MD, PhD, King's British Heart Foundation Centre, King's College London, 125 Coldharbour Ln, London SE5 9NU, UK. E-mail manuel.mayr@kcl.ac.uk

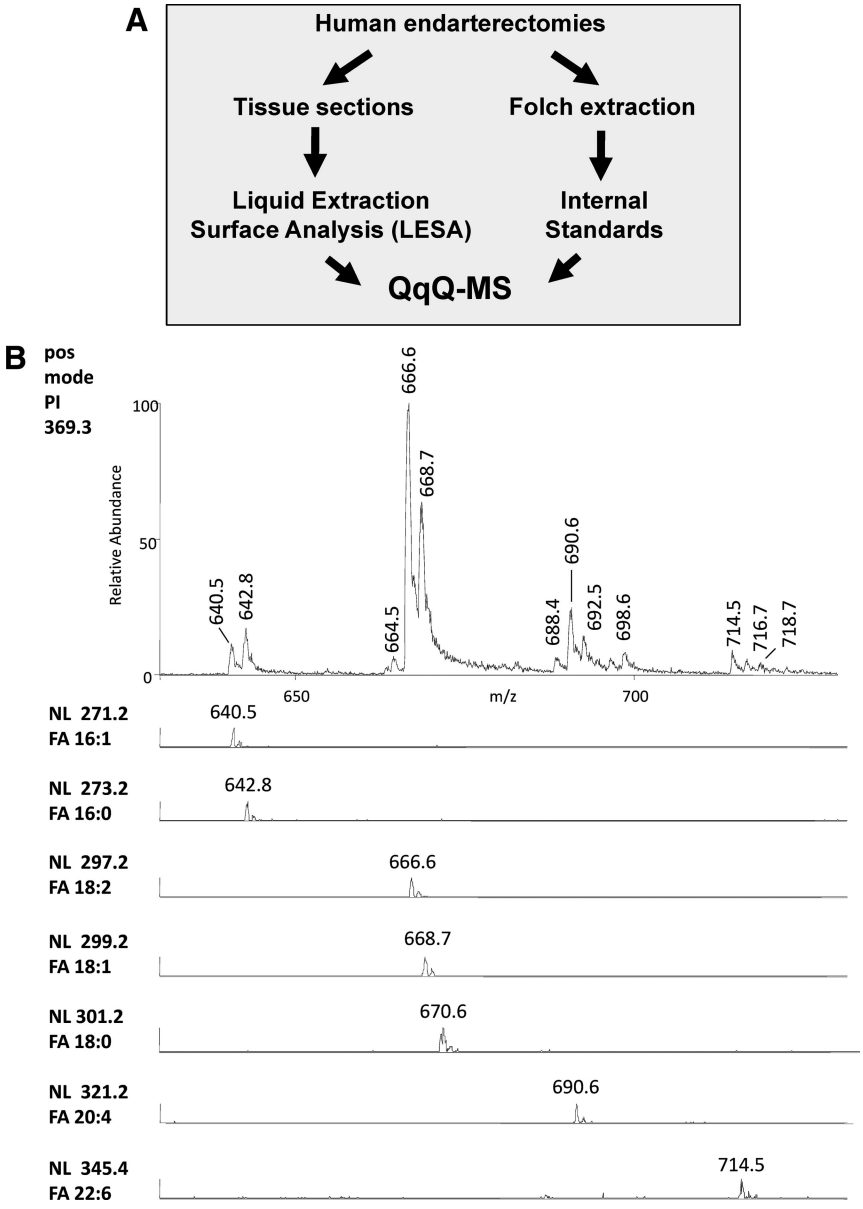

Figure 1. Workflow. **A**, Using a QqQ-MS, lipids in human endarterectomies were analyzed directly from tissue sections (LESA) or in Folch extracts. **B**, Example for a combination of PI scan (mass-to-charge ratio [m/z] 369.3) and FA scans for ammonium adducts of fatty acids to determine cholesteryl ester (CE) species. For CE(18:0) at m/z 670.6 and CE(18:1) at m/z 668.6, the identification was hindered by a partial overlap of their peaks. Nonetheless, the presence of CE(18:0) could be clearly demonstrated by the NL of the fatty acid. FA indicates fatty acid; LESA, liquid extraction surface analysis; NL, neutral loss; PI, precursor ion; QqQ-MS, triple quadrupole mass spectrometer.

provided in the online-only Data Supplement. Control radial arteries were carefully chosen to ensure that they were free of macroscopically evident vascular pathology, including atherosclerosis. Samples were briefly rinsed with cold PBS to remove superficial blood, snap-frozen in liquid nitrogen, and stored at −80°C (average storage time, 3.4±1.4 years). Eight carotid plaques from symptomatic patients were dissected into stable versus unstable areas before freezing.

Liquid Extraction Surface Analysis Coupled to Nanoelectrospray Ionization MS

Frozen human plaque samples were cut at 200 μm with a rotary microtome (Microm HM560 cryostat, Thermo Scientific), placed on electrostatically charged slides (Superfrost Plus, BDH), and air dried for 15 to 30 minutes. Lipids were directly analyzed from tissue sections with an Advion TriVersa NanoMate system (Advion BioSciences) controlled by Chipsoft software version 8.1.0.928 (Advion BioSciences) coupled to a triple quadrupole mass spectrometer (QqQ-MS) (TSQ Vantage, Thermo Fisher Scientific). The solvent extraction volume was 1.5 μL (chloroform:methanol:isopropanol 1:2:4 containing 7.5 mmol/L ammonium acetate), and the dispensed volume was 1.0 μL. Solvents were sprayed through a 4.1-μm nozzle diameter chip (Advion BioSciences) at an ionization voltage of 1.2 kV and a gas pressure of 0.3 psi. The first and third quadrupoles (mass resolution, 0.7 Thomson) served as independent mass analyzers, whereas the second quadrupole was used as the collision cell (argon was used as the collision gas with a pressure of 1.0 mTorr) for tandem MS. The temperature of the ion transfer capillary was maintained at 150°C. Full MS spectra and precursor ion (PI) scans for cholesteryl esters (CEs) (PI 369.3) and phosphatidylcholines (PCs) (PI 184.1) from different plaque sections were acquired over a period of 6 minutes.

Lipid Extraction

Lipids were extracted from endarterectomies and control radial arteries (>25 mg wet weight) using an adaptation of the Folch method.[8] A detailed description is available in the online-only Data Supplement. Plasma samples were obtained from 35 patients undergoing carotid endarterectomy. Ten microliters of plasma were used for lipid extraction through an adaptation of a recently published method.[9] Details are included in the online-only Data Supplement.

Shotgun Lipidomics

Aliquots from tissue extracts were reconstituted in 500 μL chloroform:methanol 1:2 and further diluted 1:100 with chloroform:metha-

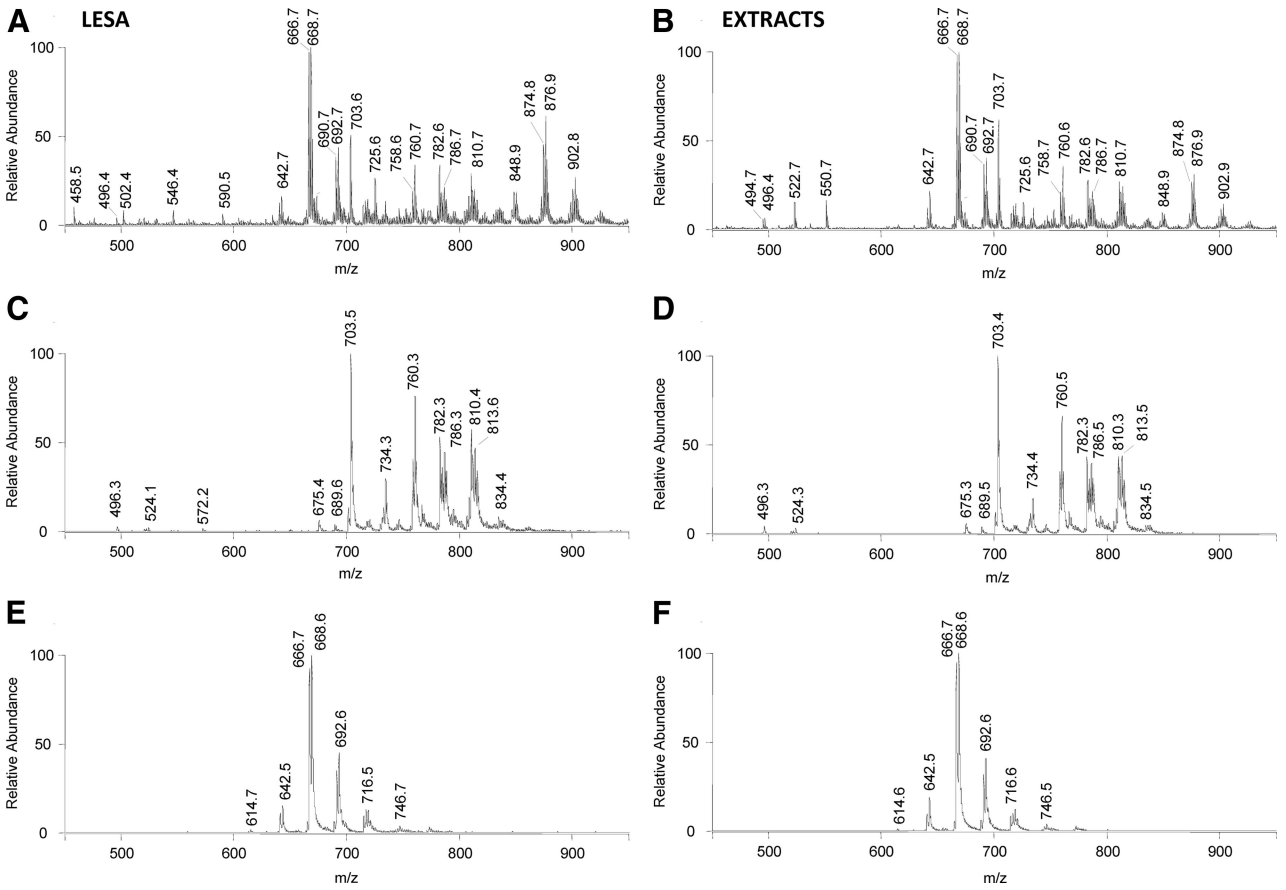

Figure 2. LESA compared to lipid extracts. The full mass spectrum in positive ion mode (**A**) and head group-specific scans for phosphatidylcholine (**C**) (PI 184.1) and CE species (**E**) (PI 369.3) from tissue sections of human endarterectomies. Note the similarity in peak numbers and correlation of signal intensities compared with tissue extracts (**B**, **D**, **F**). R^2=0.84 for the full mass spectra (**A**, **B**), R^2=0.98 for phosphatidylcholines (**C**, **D**), and R^2=0.99 for CEs (**E**, **F**). Abbreviations as in Figure 1.

nol:isopropanol 1:2:4 containing 7.5 mmol/L ammonium acetate. Plasma extracts were diluted 1:10 with chloroform:methanol:isopropanol 1:2:4 containing 7.5 mmol/L ammonium acetate for MS analysis. Just before analysis, samples were centrifuged at 12 000 rpm for 2 minutes and analyzed with a TriVersa NanoMate coupled to a QqQ-MS as described. An ionization voltage of 0.95 to 1.40 kV and a gas pressure of 1.25 psi were used.[10] Full MS spectra were acquired over a 1-minute period of signal averaging in both positive and negative profile modes. The intensity of the full MS in positive mode was 1 magnitude higher than the one in negative ion mode. For neutral loss (NL) and PI scans, the collision gas (argon) pressure was set at 1.0 mTorr; the collision energy was chosen depending on the classes of lipids. Spectra were automatically acquired with rolling scan events by a sequence subroutine operated under Xcalibur version 2.0.7 software (Thermo Fisher Scientific). The different NL and PI scans were set according to Brugger et al[11] or Han and Gross[12,13] (online-only Data Supplement Table 1). The main classes of lipids in positive ion mode were phosphatidylethanolamine/lysophosphatidylethanolamine, phosphatidylserine/lysophosphatidylserine, CE, triacylglycerol, PC/lysoPC (lPC), and sphingomyelin (SM). The PI scan of the acetate ion of the most abundant PC species in the negative ion mode was used for the identification of PC-derived fatty acids. The same parent ion scan at 184.1 was used for the identification of SMs, but the nitrogen rule allowed a discrimination of these 2 lipid classes. SMs with 2 nitrogen atoms appear at odd mass-to-charge ratio (m/z) values, whereas PC signals occur at even m/z values.[11] To further separate PCs from SMs, SMs were identified in negative ion mode by PI scan at m/z 168.0[11] (online-only Data Supplement Figure 1). For lipid quantification, 392 pmol of CE 19:0 (Avanti Polar Lipids) was added to 100 μL of each sample as an internal standard and analyzed for 2 minutes using a PI scan at m/z 369.3. The coefficient of variation for these measurements was <10% in 58% (53%) of the analytes, 10% to 20% in 18% (28%), 20% to 40% in 5% (5%), and >40% in the remainder for intraday (interday) measurements. For quantification of PC, lPC, and SM species, 52 pmol PC(17:0/17:0), 46.4 pmol/μL lPC(19:0), and 61.2 pmol SM(d18:1/12:0) were added per 100-μL sample (all Avanti Polar Lipids) and analyzed for 2 minutes using a PI scan at m/z 184.1.

Data Processing

QqQ-MS data were analyzed with Xcalibur version 2.0.7 software. Lipid identifications were based on their characteristic head groups and corresponding fatty acids by the LipidMaps database and Lipid MS Predictor version 1.5 (available at www.lipidmaps.org). For quantitation, a peak list was generated and imported into LIMSA version 1.0 software[14] using the following settings: linear fit; offset, 0; peak full width at half maximum, 0.5; and sensitivity, 0.1.

Nomenclature

We followed the designations and abbreviations recommended by the International Union of Pure and Applied Chemistry (www.chem.qmul.ac.uk/iupac/lipid). Glycero- and glycerophospholipids were named with shorthand notification, and numbers separated by colons refer to carbon chain length and number of double bonds. The composition of the side chains for the glycero- and glycerophospholipids were not assigned and were used randomly for glycerolipids. For glycerophospholipids, the unsaturated fatty acid was set on *sn*-1 position and the saturated on *sn*-2. Sphingolipids are presented in the order of long-chain base and *N*-acyl substituent.

Statistical Analysis

Statistical analysis was performed using the Student *t* test or ANOVA and Scheffé post hoc test. A $P<0.05$ was considered significant. Principal component analysis (PCA) was performed in Matlab version 2009a (The Mathworks Ltd). Capacity of each lipid to differentiate plaque or plasma samples was assessed using the out-of-bag estimates of feature importance provided by the TreeBagger class for Matlab. Data were normalized by expressing individual lipid intensities as percentages of accumulative intensities in each lipid class.

Results

Workflow Overview

Using a QqQ-MS, 2 different approaches were compared (Figure 1A): (1) liquid extraction surface analysis (LESA) for direct extraction of plaque lipids from tissue sections[15,16] and (2) shotgun lipidomics as described by Han and Gross[12] for the analysis of tissue extracts. First, a full MS scan in positive and negative ion mode was acquired. Then, PI and NL scans characteristic for different lipid classes unambiguously identified certain lipids by their characteristic MS/MS product ions (see example for CE identification in Figure 1B).

LESA Versus Tissue Extracts

For LESA, frozen human carotid endarterectomy samples were cut into thin sections without optimal cutting temperature compound to avoid contamination with polyethylene glycol. A 1.5-μL extraction solution was sufficient to provide a stable spray for >10 minutes. The signals within the lipid-relevant m/z range of 400 to 1000 in the full MS scan (Figure 2A) were comparable to the ones obtained by shotgun lipidomics from tissue extracts (Figure 2B). Additionally, the lipid class-specific head group scans (see Figure 2C and 2D for PI 184.1 for lPC, PC, and SMs and Figure 2E and 2F for PI 369.3 for CEs) showed similar peaks and signal intensities (see Figure 2C and 2E for tissue sections and Figure 2D and 2F for tissue extracts). Notably, lPC species within the m/z range of 490 to 540 were detected in tissue sections as well as in tissue extracts, confirming that these degradation products are present in human atherosclerotic plaques and are not artifacts of the extraction procedure.

Identification of Plaque-Lipids

A comparative lipid analysis of radial arteries and carotid and femoral endarterectomies was performed. Patient clinical characteristics are provided in online-only Data Supplement Table 2. Six scans in positive ion mode and 14 in negative ion mode resulted in the identification of 150 different lipid species (online-only Data Supplement Tables 3 and 4) of which 24 were detected in atherosclerotic plaques only (Table 1). Triacylglycerols accounted for the few prominent signals between m/z 790 and 930 in the full MS of radial arteries (C1 to C3 in Figure 3A). In contrast, the full MS scan of endarterectomy samples was dominated by CE, SM, PC, and triacylglycerol species (P1 to P3 in Figure 3A). Scans for specific lipid head groups detected lPCs, PCs, lysophosphatidylethanolamine, phosphatidylethanolamines, lysophosphatidylserines, SMs, CEs, and triacylglycerols. Unlike previous studies in human aortas,[17,18] phosphatidylserine species were also identified. Scans for acylcarnitine, phosphatidylinositol, phosphatidylinositol-phosphates, phosphatidylinositol 4,5-biphosphate, sulfatides, acylCoA, ceramides, and cerebrosides did not reveal strong enough signals for these lipid classes in our shotgun lipidomics analysis.

Table 1. Plaque-Enriched Lipids

	Lipid Species	m/z
Positive ion mode		
lPS	lPS(20:0)	554.3
PS	PS(38:5)	810.5
	PS(38:2)	816.5
lPC	lPC(14:0)	468.3
	lPC(0–16:0)	482.3
	lPC(0–18:0)	510.3
	lPC(18:2)	520.3
	lPC(22:5)	570.4
	lPC(22:4)	572.3
PC	PC(0–16:0/22:5)	794.5
	PC(18:0/20:3)	812.7
CE	CE(10:0)	558.5
	CE(14:0)	614.6
	CE(16:1)	640.6
	CE(18:3)	664.6
	CE(18:1)	668.7
	CE(22:6)	714.5
	CE(22:5)	716.7
	CE(22:4)	718.6
	CE(22:3)	720.7
PE	PE(38:3)	770.8
Negative ion mode		
SM	SM(d18:1/14:0)	709.7+733.4
	SM(d18:1/15:0)	723.8+747.5
	SM(d18:0/15:0)	749.5

CE indicates cholesteryl ester; lPC, lysophosphatidylcholine; m/z, mass-to-charge ratio; PC, phosphatidylcholine; PE, phosphatidylethanolamine; SM, sphingomyelin.

Quantitation of Plaque-Lipids

A comparison between control arteries and endarterectomies revealed that the signal intensities of the head group scans for lPCs, PCs, and SMs differed by 1 order and for CE by 2 orders of magnitude (Figure 3B). To calculate the total amount of CEs, lPCs, PCs, and SMs in atherosclerotic plaques, authentic standards were spiked into the samples. The highest accumulation was observed for CE species (Table 2). The average CE content was 23.9 mg/g in plaques compared to 0.2 mg/g in control arteries (Figure 4A). As expected, oleic acid (18:1) and linoleic acid (18:2) were the most common fatty acids (online-only Data Supplement Table 5). The relative distribution of CEs identified in plaque and control arteries is depicted in Figure 4B.

Comparison of Carotid Endarterectomies

Next, we compared the lipid content of carotid endarterectomy samples from closely matched symptomatic and asymptomatic patients (n=6 per group). Their clinical characteris-

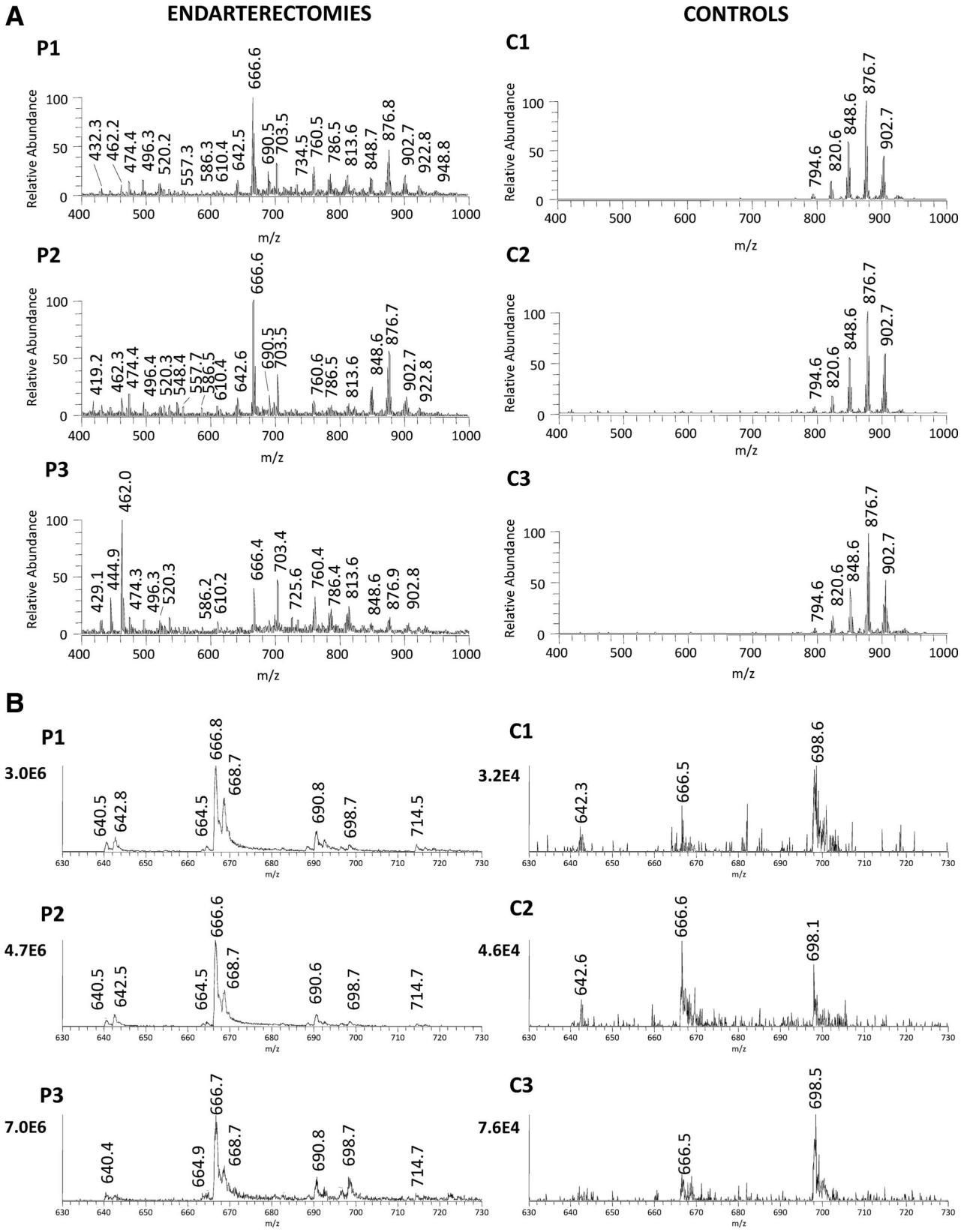

Figure 3. Endarterectomies versus radial arteries. **A**, Full mass spectra in positive ion mode for 3 control radial arteries (C1 through C3) and 3 endarterectomies (P1 through P3). **B**, Comparison among patient samples P1, P2, and P3 and control samples C1, C2, and C3 for their CE head group scan at m/z 369.3. The values next to the y-axis are the signal intensities. Abbreviations as in Figure 1.

Table 2. Total Amount of CE, IPC, PC, and SM Species in Plaques and Control Arteries

Lipid Class	Endarterectomies (n=3)	Controls (n=3)	Δ*
CE	23.95±3.50	0.20±0.10	119.5
IPC	0.36±0.15	0.02±0.01	18.0
PC	3.82±1.05	0.73±0.17	5.2
SM	4.05±1.36	0.27±0.03	15.0

Data are presented as mean±SEM milligram/gram tissue. The total amount was calculated from the femtomole- and picomole-per-microliter values provided in online-only Data Supplement Table 5 using the average molecular weight from all detected species of each lipid class. Abbreviations as in Table 1.

*Fold enrichment in plaques (n=3) compared with control specimens (n=3).

tics are provided in online-only Data Supplement Table 6. PCA was performed to investigate the global variation of the patient samples in their lipid profiles. The distance between symptomatic and asymptomatic patients in PCA was negligible, although the 2 first principal components captured 97% of the variance (online-only Data Supplement Figure 2). Given the heterogeneity of carotid endarterectomy samples, plaques excised from symptomatic and asymptomatic patients may share similar features. To reduce heterogeneity, in another cohort of patients (online-only Data Supplement Table 7), the stable area of the plaque with no signs of rupture was carefully separated from the unstable area in which there was "ulceration" of the surface with or without thrombosis and intraplaque hemorrhage, thereby providing an internal control for each sample and minimizing interpatient variability. Quantitative data for all lipid measurements in stable and unstable plaque areas are included as online-only Data Supplement Table 8. The 10 most differentially expressed species from 4 different lipid classes were sufficient to separate stable and unstable areas within the same lesion in PCA (Figure 5). No separation was obtained with individual lipid classes (Figure 5).

Comparison to Plasma Lipids

Plasma samples of 35 patients undergoing carotid endarterectomies were analyzed by shotgun lipidomics. Their clinical characteristics are provided in online-only Data Supplement Table 9. Compared with recent studies on plasma lipids using either direct injection[10] or ultraperformance liquid chromatography MS,[9,19] twice as many CE species were detected by our shotgun approach. In total, 10 CEs, 9 SMs, 8 lPCs, and 31 PCs were identified (online-only Data Supplement Table 10). As expected, plaque and plasma samples were well separated by PCA (Figure 6A). The main lipids contributing to this separation were CE, PC, and SM species (Figure 6B). The quantitative values of the different species and their relative distribution are provided in online-only Data Supplement Figures 3 through 6. In agreement with previous reports,[20] CE(18:2) constituted ≈40% of all CE species in plasma from patients with endarterectomies but accounted for only 28% in

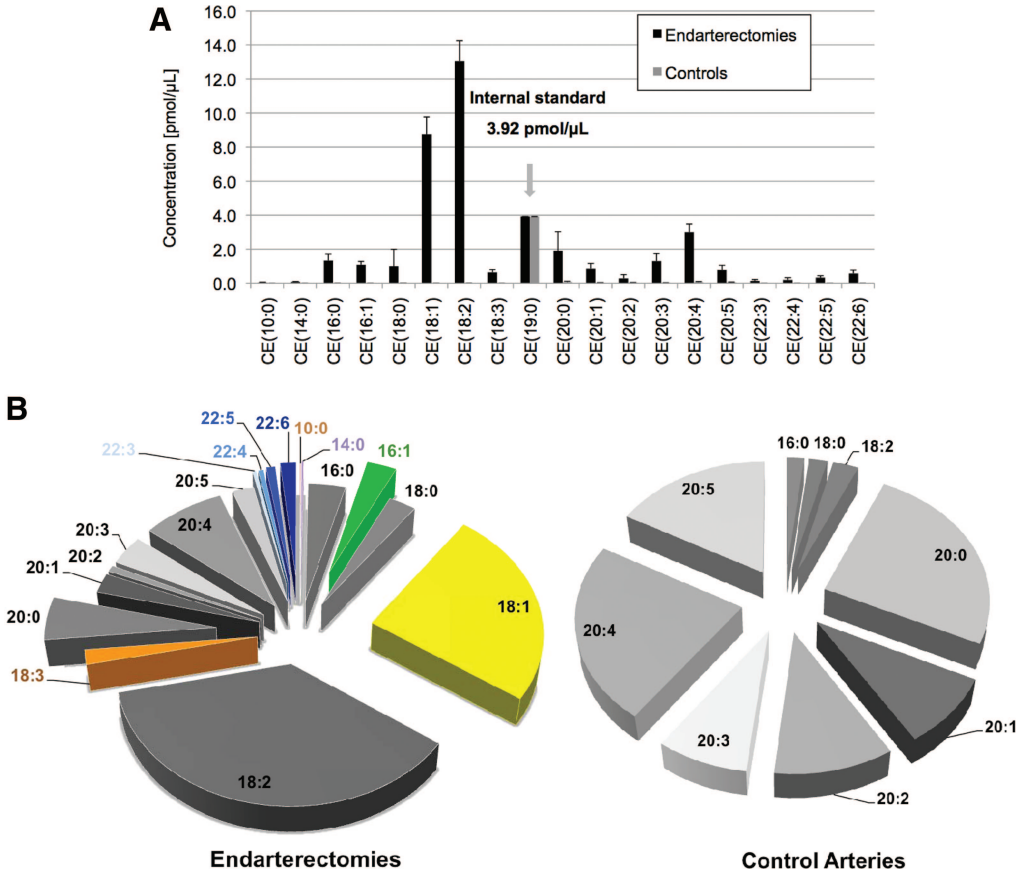

Figure 4. Plaque-enriched CE species. **A**, Quantification of CE species in plaque and control samples with CE(19:0) as internal standard. **B**, Relative distribution of CE in atherosclerotic plaques compared with control arteries. Plaque-specific CE species are highlighted in color. Abbreviation as in Figure 1.

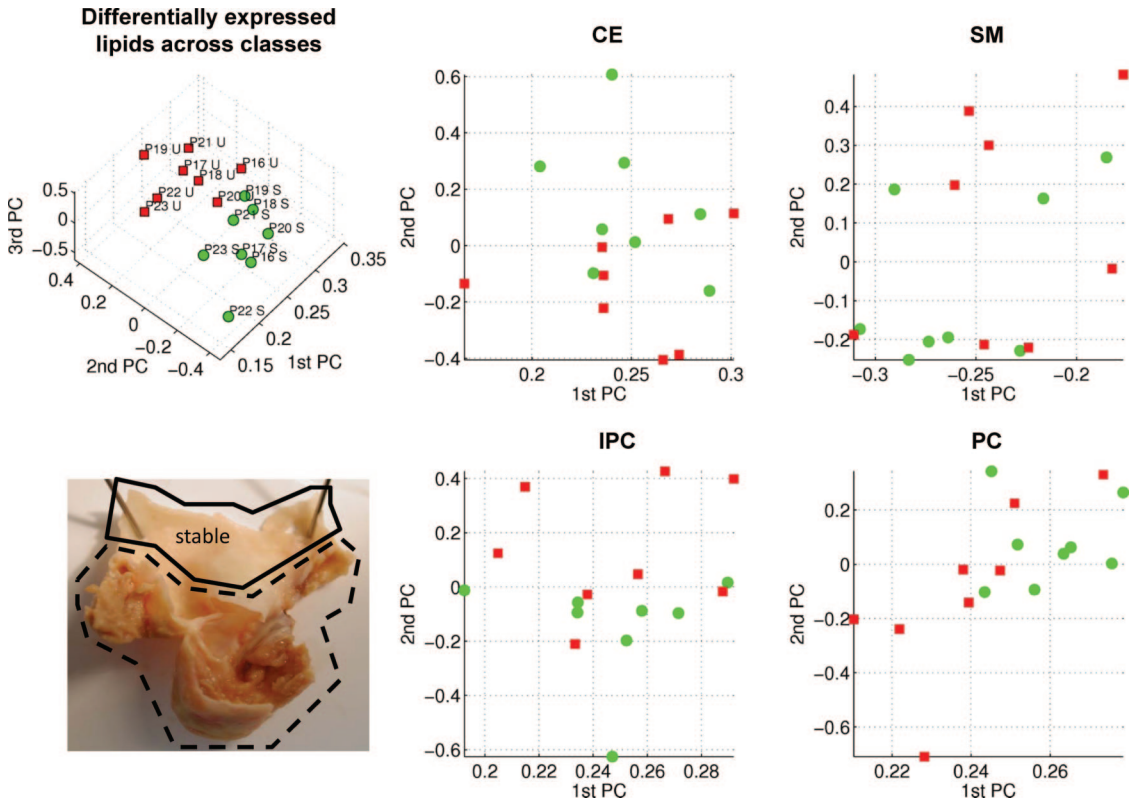

Figure 5. Plaque heterogeneity. Principal component analyses for lipid profiles of unstable and stable areas of the same symptomatic plaques (inset, macroscopic classification). The green circles denote stable areas and the red squares, unstable areas of the same lesion. The numbers correspond to the patients in online-only Data Supplement Table 7. lPC indicates lysophosphatidylcholine; P, patients; PC, phosphatidylcholine; S, stable; SM, sphingomyelin; U, unstable.

plaques. In contrast, the relative contribution of CE(18:1) to the total CE content was similar in plaques and plasma (≈30%). Polyunsaturated CE with long-chain fatty acids, which were previously undetectable in plasma by thin-layer chromatography,[20] showed the strongest relative enrichment in plaques among all CE species analyzed (Figure 6A, Table 3). Their relative contribution to the total CE content declined in unstable compared to stable regions (ie, CE(20:3) [$P<0.006$]).

Systems-Wide Analysis of Plaque Lipids

Lipid expression similarity in plaques from asymptomatic and symptomatic patients as well as in stable and unstable areas within the same lesion was inferred using Pearson correlation coefficients and visualized as networks where nodes correspond to lipids and edges link correlated pairs (Pearson correlation coefficient ≥0.70). Clusters of interlinked lipids were identified using an unbiased network clustering algorithm.[21] This systems-wide analysis revealed plaque-specific lipid signatures consisting of 19 lipid species in asymptomatic-symptomatic lesions (Figure 7A), 12 lipid species in stable-unstable plaque areas (Figure 7B), and 33 common lipid species that were differentially linked in the 2 networks (Figure 7A and 7B). Network clustering demonstrated that lipid species belonging to the same class were more likely to be linked in the stable-unstable network of different areas within the same lesions [eg, CE(22:4), CE(22:5), CE(22:6)]. These connectivity patterns were not observed in the asymptomatic-symptomatic network comparing plaques from different patients. Thus, the lipid composi-

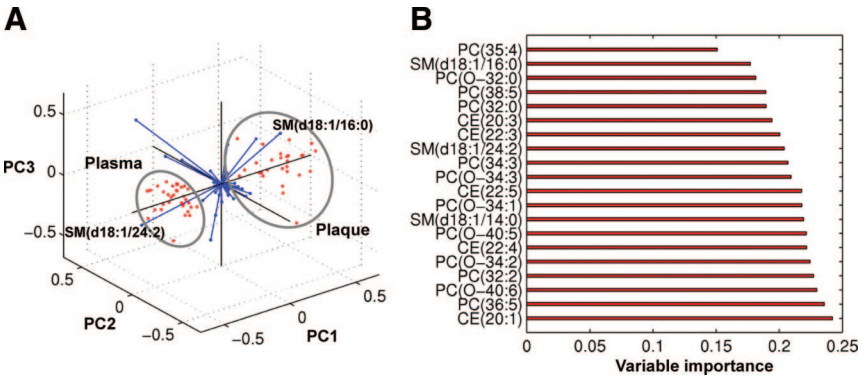

Figure 6. Differential lipid profile in plaque and plasma samples. **A**, Principal component analysis of 87 lipid species across plaque (n=28) and plasma (n=35). Magnitude and sign of the contribution of each lipid to the first 3 principal components is visualized as blue lines. **B**, Lipid importance for differentiating plaque and plasma samples. Higher values are indicative of greater importance. Abbreviations as in Figure 5.

Table 3. Quantitation of Plaque and Plasma CEs

CE Species	Asymptomatic, % (n=6)	Symptomatic, % (n=6)	P*	Unstable, % (n=8)	Stable, % (n=8)	P†	Plasma, % (n=35)	P§
CE(10:0)	0.0±0.013	0.1±0.033	0.480	0.2±0.083	0.1±0.025	0.283	0.0±0.000	<0.001‖
CE(14:0)	0.4±0.036	0.4±0.047	0.689	0.5±0.173	0.3±0.031	0.425	0.3±0.016	0.015‖
CE(16:0)	7.1±0.598	7.1±0.204	0.967	6.3±0.284	6.2±0.190	0.857	6.9±0.167	0.209
CE(16:1)	2.8±0.498	2.5±0.211	0.698	2.8±0.393	2.4±0.187	0.189	2.6±0.199	0.769
CE(18:0)	1.0±0.644	1.1±0.738	0.954	2.1±0.799	0.0±0.000	0.036‖	0.0±0.000	0.001‖
CE(18:1)	25.4±1.831	26.0±1.740	0.826	26.3±1.885	29.2±1.247	0.154	30.0±0.446	0.001‖
CE(18:2)	31.8±3.166	28.1±1.755	0.326	31.2±1.655	27.8±1.745	0.147	41.4±0.766	<0.001‖
CE(18:3)	1.3±0.208	1.2±0.222	0.894	1.7±0.242	1.4±0.095	0.145	1.9±0.174	0.026‖
CE(20:0)	6.4±1.323	6.7±1.297	0.854	3.7±0.589	2.2±0.458	0.058	0.5±0.054	<0.001‖
CE(20:1)	3.3±0.131	4.4±0.908	0.260	2.2±0.117	2.1±0.508	0.789	0.0±0.000	<0.001‖
CE(20:2)	1.1±0.155	2.3±0.732	0.146	1.9±0.447	1.9±0.311	0.991	0.0±0.000	<0.001‖
CE(20:3)	3.1±0.380	4.6±0.690	0.082	3.6±0.345	6.7±0.777	0.006‖	0.0±0.000	<0.001‖
CE(20:4)	9.0±0.978	6.7±0.947	0.114	8.5±0.960	9.4±0.850	0.325	12.6±0.738	<0.001‖
CE(20:5)	3.7±0.758	3.8±0.757	0.935	3.5±0.343	3.3±0.302	0.617	2.5±0.235	0.002‖
CE(22:3)	0.4±0.070	0.6±0.078	0.064	0.8±0.359	0.8±0.171	0.974	0.0±0.000	<0.001‖
CE(22:4)	0.4±0.086	0.8±0.152	0.037‖	0.8±0.175	1.5±0.311	0.053	0.0±0.000	<0.001‖
CE(22:5)	0.8±0.168	1.5±0.414	0.145	1.8±0.236	1.9±0.325	0.525	0.0±0.000	<0.001‖
CE(22:6)	1.9±0.267	2.0±0.242	0.738	2.2±0.425	2.7±0.404	0.262	1.3±0.081	<0.001‖

Data are presented as mean±SE. Abbreviation as in Table 1.

*P values from unpaired t test for differences between asymptomatic and symptomatic patients.

†P values from paired t test for differences between stable and ruptured (unstable) areas of the same plaque.

§P values from unpaired t test for differences of all plaque (n=28) and plasma samples (n=35).

‖Significant at $P<0.05$.

tion and connectivity between lipid species may contribute toward a better characterization of atherosclerotic lesions.

Discussion

Although lipids of human atherosclerotic plaques have been analyzed previously, target-focused measurements restricted to individual lipid classes remain insufficient to reveal the global lipid imbalances in atherosclerosis. This study demonstrates the integration of advanced MS toward a better characterization of the lipid composition in atherosclerosis.

QqQ-MS

The different scan options of the QqQ-MS can resolve isobaric lipids from different lipid subclasses and detect less-prominent species in the presence of high-abundant lipids. Notably, LESA allowed a rapid analysis of plaque lipids directly from tissue sections without time- and labor-intensive sample preparation. To the best of our knowledge, this is the first time that LESA was used in combination with a QqQ-MS for lipid profiling. The signals as well as the signal intensities were comparable to shotgun lipidomics of tissue extracts (Figure 2). For quantification, lipid extracts were spiked with class-specific internal standards. Because specificity is achieved by the characteristic head group scans on the QqQ-MS, only a single standard per lipid class is required. Thus, the shotgun lipidomics approach is less expensive compared with other MS-based lipid analysis techniques and is applicable to tissue sections as well as to extracts.

Lipids in Atherosclerosis

Cholesterol within the vasculature accumulates as CE as a droplet either in the cytosol or in lysosomes.[22] Infiltrating low-density lipoprotein (LDL) particles contain a CE-rich core, with linoleic acid [CE(18:2)] as the most abundant polyunsaturated fatty acid.[23] The intimate relationship of plasma lipids, vascular matrix, and CE deposits in the arterial wall is well documented.[24–26] Currently, our knowledge at the biological level is mostly related to the classes of lipids rather than to the bioactivity of a single lipid species within these classes.[2] Yet, the actual species composition of the lipid classes is likely to be an important atherogenic factor; that is, LDL particles enriched with monounsaturated cholesteryl oleate [CE(18:1)] are typically larger and more active in binding to arterial proteoglycans, thereby favoring retention and subsequent formation of early atherosclerotic lesions.[27] In comparison, LDL particles enriched with polyunsaturated cholesteryl linoleate are thought to be less atherogenic.

Shotgun Lipidomics of Plaques

In total, 150 lipid species were identified in plaques. The lipid classes accounting for the major differences between control and diseased arteries were CEs, SMs, lPCs, and PCs. Remarkable differences were observed for the relative amount of CEs with linoleic acid and other polyunsaturated fatty acids like arachidonic acid [CE(20:4)] and eicosapentaenoic acid [CE(20:5)] compared to control arteries (Figure 4). The relative decrease in polyunsaturated fatty acids coupled with an excess in linoleic acid in human plaques could be an

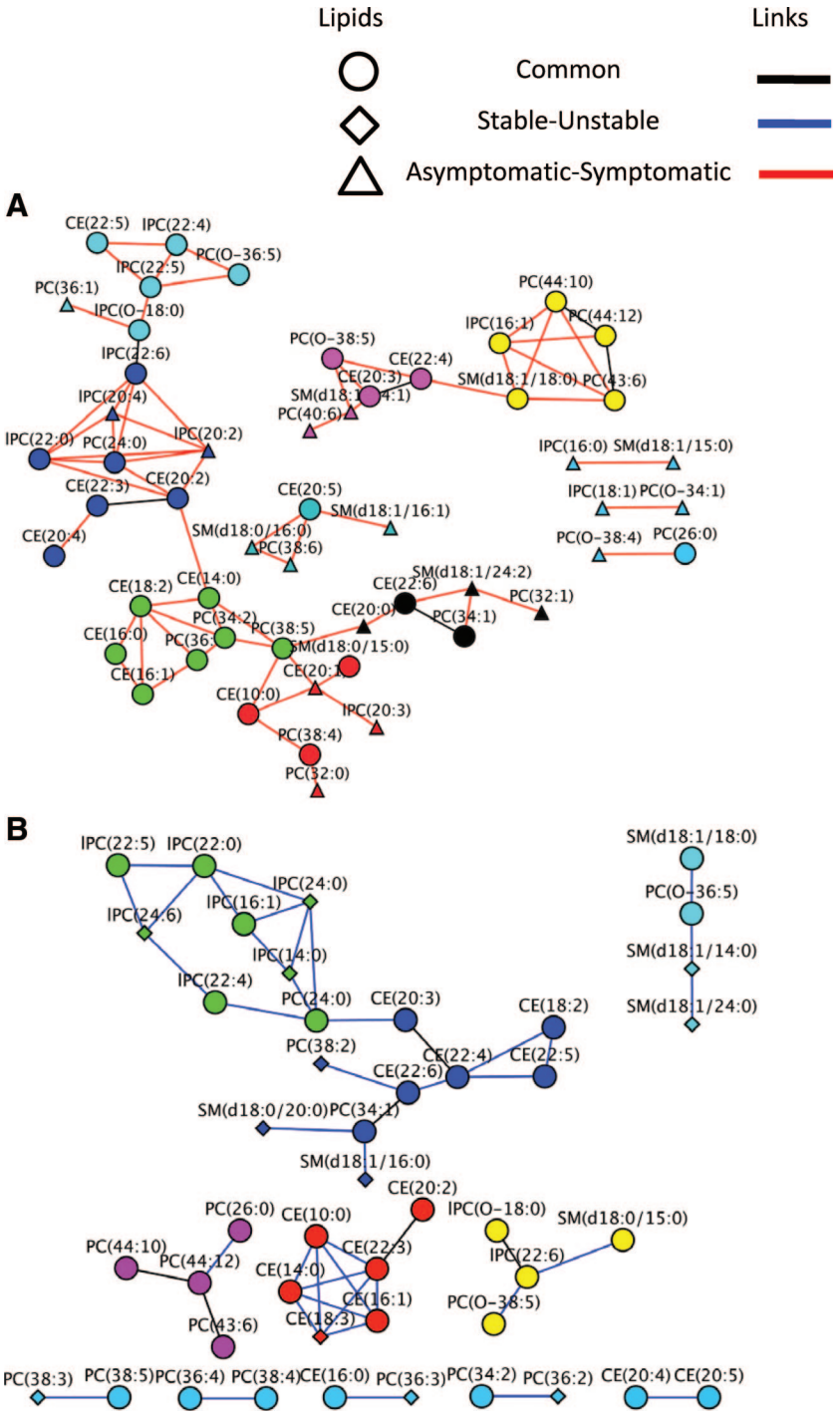

Figure 7. Systems-wide relationships between lipids involved in atherosclerosis showing lipid-lipid coexpression network where each node represents a lipid and each edge a correlation in expression between 2 lipids. Only lipid pairs with a Pearson correlation coefficient ≥0.70 were included in the network. Lipids and coexpressions specific for the asymptomatic-symptomatic phenotype (**A**) are represented as triangles and red links, respectively, whereas lipids and coexpressions specific for the stable-unstable network (**B**) are represented as diamonds and blue links. Lipids and coexpressions common to both phenotypes are represented as circles and black edges. Lipid colors correspond to unique clusters computed with an unbiased network clustering algorithm.[21] Abbreviations as in Figures 1 and 5.

indicator for altered substrate availability for inflammatory mediators and mediators of resolution (lipoxins, resolvins, and protectins).[28] A simple, rapid macroscopic method of classification based on the definitions of plaque progression and instability by Stary et al[29] was used to differentiate unstable versus stable segments of the same plaque (Figure 5).[30,31] In the present comparison, where each patient serves as his or her own control, the lipidomics approach was most successful and provided insights into the lipid heterogeneity within atherosclerotic plaques. Consistent with previous reports,[20] CE(18:2) was the major CE species in atherosclerosis, and the relative distribution of most CEs was comparable to results obtained by thin-layer chromatography, providing independent validation of the quantitative accuracy of our approach. The sensitivity of shotgun lipidomics, however, allowed the identification of additional CE species and other lipid classes, such as lPCs (a by-product of LDL oxidation and formed by the enzymes phospholipase A_1, phospholipase A_2, or lecithin:cholesterol acyltransferase) and SMs (a ubiquitous component of cell membranes and of the LDL surface). Plasma lipoproteins are the main source for SMs,[18] and high SM plasma levels were associated with coronary artery disease.[32] SM and its hydrolyzing enzyme SMase are believed to mediate biological effects, but the mechanistic links

between SM and atherosclerosis remain elusive.[33] SMs with long-chain fatty acids were substantially lower in plaques compared with plasma, whereas certain SM species [ie, SM(d18:1/16:0) and SM(d18:1/14:0)] were enriched, supporting the hypothesis that they are either selectively retained or de novo synthesized in atherosclerotic plaques.[34] Similarly, the enrichment of lPCs[35] is supposed to contribute to the pathogenesis of atherosclerosis and, in particular, inflammation.[36]

Systems-Wide Network Analysis

The postgenomic shift in paradigm acknowledges the fact that biological systems are pleiotropic and interconnected.[37] Similarly, systemic relationships between lipid classes in atherosclerotic lesions are important for understanding genotype-phenotype relationships[38] and for working toward a lipid signature for risk prediction, early diagnosis, and personalized treatment of this disease. Previous studies enabled only a partial analysis of plaque lipids and mainly focused on LDL cholesterol[24,39–41] and its derivatives.[41,42] There are also publications about individual lipid classes in atherosclerotic plaques (ie, isoprostanes,[23] lipid mediators,[4] lPCs,[35] oxidized PCs,[43] phospholipids[44]), but no comprehensive comparison between control and diseased arteries across different lipid classes has been performed to date. Manicke et al[7] recently applied desorption electrospray ionization MS to atherosclerotic plaque tissue. As proof of principle, lipid profiling was performed on a single human plaque in positive and negative ion mode, and 26 lipid species were identified. Our shotgun lipidomic approach identified all of the 26 lipids except SM(22:0) (online-only Data Supplement Tables 3 and 4). Moreover, we were able to show that 16 of the 26 lipids in the former study were present in control arteries and, therefore, are not plaque specific. Using a network approach, we demonstrate that homogeneous lipid clusters were identified in the stable-unstable network from the same lesion (Figure 7) and that sampling differentially expressed species across lipid classes improves the separation in PCA (Figure 5).

Limitations

Although MS has proven a valuable tool for comparative lipid analysis, minor components like signaling molecules (sphingosine-1-phosphate[45] or isoprostanes) or oxidized lipids remain undetected. Chromatographic separation would be essential to analyze these scarce lipid species. Additionally, modified lipids with alterations in the characteristic head groups and free cholesterol and other species, which do not readily ionize by electrospray ionization, were not detected in our analysis. Finally, LESA only provides a qualitative comparison of plaque lipids. Lipid extracts have to be spiked with authentic standards for quantitation.

Conclusions

To our knowledge, this study is the most comprehensive MS analysis of the lipid content in human atherosclerotic plaques to date. An in-depth comparison of the lipid composition in different atherosclerotic lesions combined with systems-wide network analysis unraveled plaque-specific lipid signatures. In the future, these advanced technologies could be exploited for diagnostic purposes or as a platform for drug screening.

Sources of Funding

This work was supported by grants from the British Heart Foundation and Oak Foundation. Prof Mayr is a Senior Research Fellow of the British Heart Foundation.

Disclosures

Mr Baumert and Dr Allen are employees of Advion BioSciences.

References

1. Williams KJ, Tabas I. The response-to-retention hypothesis of early atherogenesis. *Arterioscler Thromb Vasc Biol*. 1995;15:551–561.
2. Hu C, van der Heijden R, Wang M, van der Greef J, Hankemeier T, Xu G. Analytical strategies in lipidomics and applications in disease biomarker discovery. *J Chromatogr B Analyt Technol Biomed Life Sci*. 2009;877:2836–2846.
3. Kim SH, Lee ES, Lee JY, Lee ES, Lee BS, Park JE, Moon DW. Multiplex coherent anti-stokes Raman spectroscopy images intact atheromatous lesions and concomitantly identifies distinct chemical profiles of atherosclerotic lipids. *Circ Res*. 2010;106:1332–1341.
4. Brezinski DA, Nesto RW, Serhan CN. Angioplasty triggers intracoronary leukotrienes and lipoxin A4. Impact of aspirin therapy. *Circulation*. 1992;86:56–63.
5. Gerszten RE, Wang TJ. The search for new cardiovascular biomarkers. *Nature*. 2008;451:949–952.
6. Mayr M. Metabolomics: ready for the prime time? *Circ Cardiovasc Genet*. 2008;1:58–65.
7. Manicke NE, Nefliu M, Wu C, Woods JW, Reiser V, Hendrickson RC, Cooks RG. Imaging of lipids in atheroma by desorption electrospray ionization mass spectrometry. *Anal Chem*. 2009;81:8702–8707.
8. Folch J, Lees M, Sloane Stanley GH. A simple method for the isolation and purification of total lipides from animal tissues. *J Biol Chem*. 1957;226:497–509.
9. Laaksonen R, Katajamaa M, Paiva H, Sysi-Aho M, Saarinen L, Junni P, Lutjohann D, Smet J, Van CR, Seppanen-Laakso T, Lehtimaki T, Soini J, Oresic M. A systems biology strategy reveals biological pathways and plasma biomarker candidates for potentially toxic statin-induced changes in muscle. *PLoS One*. 2006;1:e97.
10. Graessler J, Schwudke D, Schwarz PE, Herzog R, Shevchenko A, Bornstein SR. Top-down lipidomics reveals ether lipid deficiency in blood plasma of hypertensive patients. *PLoS One*. 2009;4:e6261.
11. Brugger B, Erben G, Sandhoff R, Wieland FT, Lehmann WD. Quantitative analysis of biological membrane lipids at the low picomole level by nano-electrospray ionization tandem mass spectrometry. *Proc Natl Acad Sci U S A*. 1997;94:2339–2344.
12. Han X, Gross RW. Global analyses of cellular lipidomes directly from crude extracts of biological samples by ESI mass spectrometry: a bridge to lipidomics. *J Lipid Res*. 2003;44:1071–1079.
13. Han X, Gross RW. Shotgun lipidomics: electrospray ionization mass spectrometric analysis and quantitation of cellular lipidomes directly from crude extracts of biological samples. *Mass Spectrom Rev*. 2005;24:367–412.
14. Haimi P, Uphoff A, Hermansson M, Somerharju P. Software tools for analysis of mass spectrometric lipidome data. *Anal Chem*. 2006;78:8324–8331.
15. Kertesz V, Van Berkel GJ. Fully automated liquid extraction-based surface sampling and ionization using a chip-based robotic nanoelectrospray platform. *J Mass Spectrom*. 2010;45:252–260.
16. Marshall P, Toteu-Djomte V, Bareille P, Perry H, Brown G, Baumert M, Biggadike K. Correlation of skin blanching and percutaneous absorption for glucocorticoid receptor agonists by matrix-assisted laser desorption ionization mass spectrometry imaging and liquid extraction surface analysis with nanoelectrospray ionization mass spectrometry. *Anal Chem*. 2010;82:7787–7794.
17. Bottcher CJF, Van Gent CM. Changes in the composition of phospholipids and of phospholipid fatty acids associated with athersoclerosis in the human aortic wall. *J Atheroscl Res*. 1961;1:36–46.
18. Smith EB, Cantab BA. Intimal and medial lipids in human aortas. *Lancet*. 1960;276:799–803.
19. Castro-Perez JM, Kamphorst J, Degroot J, Lafeber F, Goshawk J, Yu K, Shockcor JP, Vreeken RJ, Hankemeier T. Comprehensive LC-MS(E) lipidomic analysis using a shotgun approach and its application to biomarker detection and identification in osteoarthritis patients. *J Proteome Res*. 2010;9:2377–2389.

20. Rapp JH, Connor WE, Lin DS, Inahara T, Porter JM. Lipids of human atherosclerotic plaques and xanthomas: clues to the mechanism of plaque progression. *J Lipid Res*. 1983;24:1329–1335.
21. Blondel VD, Guillaume J-L, Lambiotte R, Lefebvre E. Fast unfolding of communities in large networks. *J Stat Mech*. 2008;3:P10008.
22. Shio H, Haley NJ, Fowler S. Characterization of lipid-laden aortic cells from cholesterol-fed rabbits. III. Intracellular localization of cholesterol and cholesteryl ester. *Lab Invest*. 1979;41:160–167.
23. Mallat Z, Nakamura T, Ohan J, Leseche G, Tedgui A, Maclouf J, Murphy RC. The relationship of hydroxyeicosatetraenoic acids and F2-isoprostanes to plaque instability in human carotid atherosclerosis. *J Clin Invest*. 1999;103:421–427.
24. Brown AJ, Leong SL, Dean RT, Jessup W. 7-Hydroperoxycholesterol and its products in oxidized low density lipoprotein and human atherosclerotic plaque. *J Lipid Res*. 1997;38:1730–1745.
25. Suarna C, Dean RT, May J, Stocker R. Human atherosclerotic plaque contains both oxidized lipids and relatively large amounts of alpha-tocopherol and ascorbate. *Arterioscler Thromb Vasc Biol*. 1995;15:1616–1624.
26. Witting P, Pettersson K, Ostlund-Lindqvist AM, Westerlund C, Wagberg M, Stocker R. Dissociation of atherogenesis from aortic accumulation of lipid hydro(pero)xides in Watanabe heritable hyperlipidemic rabbits. *J Clin Invest*. 1999;104:213–220.
27. Degirolamo C, Shelness GS, Rudel LL. LDL cholesteryl oleate as a predictor for atherosclerosis: evidence from human and animal studies on dietary fat. *J Lipid Res*. 2009;50:S434–S439.
28. Serhan CN, Chiang N, Van Dyke TE. Resolving inflammation: dual anti-inflammatory and pro-resolution lipid mediators. *Nat Rev Immunol*. 2008;8:349–361.
29. Stary HC, Chandler AB, Dinsmore RE, Fuster V, Glagov S, Insull W Jr, Rosenfeld ME, Schwartz CJ, Wagner WD, Wissler RW. A definition of advanced types of atherosclerotic lesions and a histological classification of atherosclerosis. A report from the Committee on Vascular Lesions of the Council on Arteriosclerosis, American Heart Association. *Circulation*. 1995;92:1355–1374.
30. Papaspyridonos M, Smith A, Burnand KG, Taylor P, Padayachee S, Suckling KE, James CH, Greaves DR, Patel L. Novel candidate genes in unstable areas of human atherosclerotic plaques. *Arterioscler Thromb Vasc Biol*. 2006;26:1837–1844.
31. Papaspyridonos M, McNeill E, de Bono JP, Smith A, Burnand KG, Channon KM, Greaves DR. Galectin-3 is an amplifier of inflammation in atherosclerotic plaque progression through macrophage activation and monocyte chemoattraction. *Arterioscler Thromb Vasc Biol*. 2008;28:433–440.
32. Jiang XC, Paultre F, Pearson TA, Reed RG, Francis CK, Lin M, Berglund L, Tall AR. Plasma sphingomyelin level as a risk factor for coronary artery disease. *Arterioscler Thromb Vasc Biol*. 2000;20:2614–2618.
33. Auge N, Negre-Salvayre A, Salvayre R, Levade T. Sphingomyelin metabolites in vascular cell signaling and atherogenesis. *Prog Lipid Res*. 2000;39:207–229.
34. Yeboah J, McNamara C, Jiang XC, Tabas I, Herrington DM, Burke GL, Shea S. Association of plasma sphingomyelin levels and incident coronary heart disease events in an adult population: Multi-Ethnic Study of Atherosclerosis. *Arterioscler Thromb Vasc Biol*. 2010;30:628–633.
35. Thukkani AK, McHowat J, Hsu FF, Brennan ML, Hazen SL, Ford DA. Identification of alpha-chloro fatty aldehydes and unsaturated lysophosphatidylcholine molecular species in human atherosclerotic lesions. *Circulation*. 2003;108:3128–3133.
36. Matsumoto T, Kobayashi T, Kamata K. Role of lysophosphatidylcholine (LPC) in atherosclerosis. *Curr Med Chem*. 2007;14:3209–3220.
37. Barabasi AL, Oltvai ZN. Network biology: understanding the cell's functional organization. *Nat Rev Genet*. 2004;5:101–113.
38. Dreze M, Charloteaux B, Milstein S, Vidalain PO, Yildirim MA, Zhong Q, Svrzikapa N, Romero V, Laloux G, Brasseur R, Vandenhaute J, Boxem M, Cusick ME, Hill DE, Vidal M. 'Edgetic' perturbation of a *C. elegans* BCL2 ortholog. *Nat Methods*. 2009;6:843–849.
39. Carpenter KL, Wilkins GM, Fussell B, Ballantine JA, Taylor SE, Mitchinson MJ, Leake DS. Production of oxidized lipids during modification of low-density lipoprotein by macrophages or copper. *Biochem J*. 1994;304(pt 2):625–633.
40. Carpenter KL, Taylor SE, van d V, Williamson BK, Ballantine JA, Mitchinson MJ. Lipids and oxidised lipids in human atherosclerotic lesions at different stages of development. *Biochim Biophys Acta*. 1995;1256:141–150.
41. Upston JM, Niu X, Brown AJ, Mashima R, Wang H, Senthilmohan R, Kettle AJ, Dean RT, Stocker R. Disease stage-dependent accumulation of lipid and protein oxidation products in human atherosclerosis. *Am J Pathol*. 2002;160:701–710.
42. Carpenter KL, Taylor SE, Ballantine JA, Fussell B, Halliwell B, Mitchinson MJ. Lipids and oxidised lipids in human atheroma and normal aorta. *Biochim Biophys Acta*. 1993;1167:121–130.
43. Davis B, Koster G, Douet LJ, Scigelova M, Woffendin G, Ward JM, Smith A, Humphries J, Burnand KG, Macphee CH, Postle AD. Electrospray ionization mass spectrometry identifies substrates and products of lipoprotein-associated phospholipase A2 in oxidized human low density lipoprotein. *J Biol Chem*. 2008;283:6428–6437.
44. Ravandi A, Babaei S, Leung R, Monge JC, Hoppe G, Hoff H, Kamido H, Kuksis A. Phospholipids and oxophospholipids in atherosclerotic plaques at different stages of plaque development. *Lipids*. 2004;39:97–109.
45. Levkau B. Sphingosine-1-phosphate in the regulation of vascular tone: a finely tuned integration system of S1P sources, receptors, and vascular responsiveness. *Circ Res*. 2008;103:231–233.

CLINICAL PERSPECTIVE

Although lipids of human atherosclerotic plaques have been analyzed previously, target-focused measurements restricted to individual lipid classes remain insufficient to reveal the global lipid imbalances in atherosclerosis. We have adapted a liquid extraction-based surface sampling device for the analysis of plaque lipids from tissue sections. For quantitation, shotgun lipidomics was performed on lipid extracts using the different scan options of a triple quadrupole mass spectrometer. In total, 150 lipid species from 9 different classes were identified, of which 24 were detected in endarterectomies only. A comparison of 28 carotid endarterectomy specimens revealed lipid signatures of symptomatic-asymptomatic lesions as well as stable-unstable plaque areas. This comprehensive analysis of plaque lipids highlights the importance of measuring individual lipid species rather than lipid classes to obtain insights into the lipid heterogeneity within atherosclerotic lesions.